

# Production of hot nuclei in Fermi energy domain: from peripheral to central collisions.

M. Veselsky <sup>\*†</sup>

Cyclotron Institute, Texas A&M University, College Station, TX 77843.

February 5, 2020

## Abstract

The production of highly excited nuclei in the Fermi energy domain is investigated. A phenomenological approach, based on the exciton model, is used for the description of pre-equilibrium emission. A model of deep inelastic transfer is employed for the peripheral collisions in the post-pre-equilibrium stage. An approach to describe more central collisions is proposed. A geometric overlap formula is employed in a way suitable for given energy domain. A simple geometric approach describing the interaction of participant and spectator zones is used to determine the incomplete fusion channel. Excitation energies of both fragments are determined. Results of the calculation are compared to available experimental data and an overall satisfactorily agreement is obtained. The model's ability to describe the production of the hot nuclei can be employed in the study of multifragmentation and/or in the production of rare beams.

A detailed knowledge of the production mechanism of hot nuclei is desirable for the understanding of multifragmentation. The peripheral collisions of heavy ions in the Fermi energy domain demonstrate that the nucleon exchange is a dominating production mechanism of the highly excited quasiprojectiles. In more violent collisions, the processes leading to the mid-velocity emission start to play an important role. The influence of the pre-equilibrium emission and fragmentation-like processes becomes an important issue. There exists a considerable amount of experimental data from the reactions of heavy ions in the Fermi energy domain ( for review see e.g. refs. [1, 2] ). Various transport and molecular dynamics models are generally used for a theoretical description ( for review see e.g. ref. [3] and references therein ). In this article, a framework based on simple phenomenological assumptions will be presented and its ability to describe the experimental data will be demonstrated.

The pre-equilibrium emission ( PE ) is a process where fast particles are emitted prior to the equilibration of the system. Emission of pre-equilibrium particles in reactions induced by nucleons and light particles was theoretically explained using the exciton model [4] or using the master equations [5]. For reactions induced by heavy ion beams a model of nucleon exchange was developed [6]. In the present work, we use a phenomenological description [7] based on similar assumptions as the exciton model. The probability of pre-equilibrium emission is evaluated using the formula

$$P_{pre}(n/n_{eq}) = 1 - e^{-\frac{(n/n_{eq}-1)^2}{2\sigma^2}} \quad (1)$$

---

<sup>\*</sup>phone: (979)-845-1411, fax: (979)-845-1899, e-mail: veselsky@comp.tamu.edu

<sup>†</sup>On leave of absence from Institute of Physics of SASc, Bratislava, Slovakia

for  $n \leq n_{eq}$  and is assumed zero for  $n > n_{eq}$ , where  $n$  is the number of excitons at given stage and  $n_{eq}$  is the the number of excitons in the equilibrium configuration for given excitation energy. The  $\sigma$  is a free parameter. The basic assumption leading to eq. ( 1 ) is the dependence of  $P_{pre}$  on the ratio  $n/n_{eq}$  as suggested in ref. [8]. An initial exciton number is equal to the mass number of the beam. The equilibrium number of excitons is calculated according to the formula [8]

$$n_{eq} = 2 g T \ln 2 \quad (2)$$

where  $g$  is the one particle level density at the Fermi energy and  $T$  is the nuclear temperature determined as  $T^2 = U/\tilde{a}$ , where  $\tilde{a}$  is the asymptotic level density parameter and  $U$  is the excitation energy. At every emission step, a random number between zero and one is generated. If the random number is smaller than  $P_{pre}$  a pre-equilibrium particle is emitted. The emission of neutron, proton and  $\alpha$ -particle is considered and the Weisskopf-Ewing emission widths are used. The Maxwellian spectrum of kinetic energy with the apparent temperature [9]

$$T_{app} = \left[ \frac{2.5}{A_P} (E_P - V_C) \right]^{1/2} \quad (3)$$

is assumed, where  $A_P$  is the projectile mass number,  $E_P$  is the projectile energy and  $V_C$  is the Coulomb barrier. The emission angle is determined according to the formula [10]

$$\frac{d\sigma}{d\Omega} = K \exp\left(\frac{-\theta}{\Delta\theta}\right) \quad (4)$$

where  $\Delta\theta = \frac{2\pi}{kR_{CN}}$ ,  $R_{CN}$  is the radius of the compound nucleus and  $k$  is the wave number of the emitted particle. After emission, the exciton number is increased by the value obtained using the formula

$$\Delta n = A_{pre} \frac{\kappa}{\beta_{rad}} \quad (5)$$

where  $A_{pre}$  is the mass of emitted particle,  $\beta_{rad}$  is the radial velocity in the contact configuration at a given angular momentum and  $\kappa$  is a free parameter. If no pre-equilibrium emission occurs at a given emission stage, the pre-equilibrium stage is finished.

As a next step, the interaction of the projectile and target is considered. As shown in several works [11, 12], the model of deep inelastic transfer ( DIT ) describes well the peripheral collisions where the relative motion is mostly tangential. With decreasing angular momentum the radial motion becomes more intense and violent scenarios should be considered. At low energies several MeV/nucleon above the Coulomb barrier an incomplete fusion was observed by detecting evaporation residues [10, 13, 14] or fission fragments [15]. The framework of angular momentum windows was introduced by Wilczynski et al. [16]. At very high projectile energies the abrasion-ablation model [17] is used widely to describe the fragmentation phenomena. In the proposed description, different scenarios are employed depending on angular momentum. At large angular momenta, the model of deep inelastic transfer is used. In the more central collisions, where stationary di-nuclear configuration cannot be created, the framework of a geometric overlap is used. In the near-central collisions a model of Wilczynski [16] is employed.

Since pre-equilibrium emission happens prior to the fragmentation stage, it is necessary to reconstruct the post-pre-equilibrium projectile-target configuration. It is assumed, according e.g. to the conclusions of work [6] that pre-equilibrium particles are mostly emitted from the ( usually light ) projectile and propagate through the target. The emitted mass and charge are subtracted from the projectile. The excitation energy of the target is set equal to the sum of kinetic energies

of the emitted pre-equilibrium particles, in accordance to the assumption that one nucleon-nucleon collision occurs during the propagation of the particle through the target.

For every event the Monte Carlo code of Tassan-Got [11] is used. In the case when di-nuclear configuration is created, deep inelastic transfer takes place and excited quasi-projectile and quasi-target are created. In the cases, where overlap of nuclei is too deep, the more violent scenario ( here arbitrarily denoted as realistic geometric fragmentation - RGF ), is considered. The geometric overlap formula of the abrasion-ablation model [17] is used. It is clearly unrealistic to assume that the projectile propagates along straight line determined by the asymptotic value of impact parameter. Instead, a minimum distance between projectile and target in the Coulomb scattering of two point-like charges is used. Thus, one participant and one or two spectator zones are created.

The charges of the spectators are determined according to the combinatorial formula [18, 19]

$$P(Z_{iS}) = \binom{Z_i}{Z_{iS}} \binom{N_i}{N_{iS}} / \binom{A_i}{A_{iS}} \quad (6)$$

where  $i=P(T)$  for the projectile ( target ),  $A_{P(T)}$ ,  $Z_{P(T)}$ ,  $N_{P(T)}$  are the mass number, charge and neutron number of the projectile ( target ) and  $A_{P(T)S}$ ,  $Z_{P(T)S}$ ,  $N_{P(T)S}$  are mass, charge and the neutron number of the projectile ( target ) spectator. The charge of participant zone is determined assuming charge conservation.

In the Fermi energy domain one can assume that the participant zone can be captured by either projectile or target spectator zone. In order to decide between these two, the volume occupied by the neighboring nucleons within the reach of nuclear interaction ( 1 fm ) is determined in both spectators. The volume is approximated by a 1 fm thick slice of the sphere. The number of neighboring nucleons (  $A_{NS}$  ) is then determined using a normal distribution centered at the value exactly corresponding to the volume with the standard deviation equal to  $\sqrt{A_{NS}}$ . The numbers of neighboring nucleons are compared and the participant zone is captured by the spectator with more neighboring nucleons. Such a procedure reflects the saturation of the nuclear force. The capturing spectator and the captured participant zone form a very hot fragment. The other spectator is much colder. In this case, the excitation energy is determined using the formula

$$E_S^* = x A_{NS} \left( \frac{E_{P'}}{A_{P'}} - V_{C'} \right) \frac{\langle s \rangle}{\lambda} \quad (7)$$

where  $E_{P'}$  and  $A_{P'}$  are the kinetic energy and the mass number of the effective projectile after pre-equilibrium emission,  $V_{C'}$  is the Coulomb barrier,  $\langle s \rangle$  is the mean effective path of the nucleon along the spectator trajectory within the slice,  $\lambda$  is the mean free path between the nucleon-nucleon collisions in the nucleus ( a value 6 fm is chosen ) and  $x$  is a random number between zero and one.

The energy and the angle of the spectator is determined using the formula of Matsuoka et al. [20] based on the Serber approximation. The formula reads

$$\frac{d^2\sigma}{dE_a d\Omega_a} = \frac{(E_a E_b)^{1/2}}{(2\mu B_{P'} + 2m_a^2 E_{P'}/m_{P'} + 2m_a E_a - 4(m_a^3 E_{P'} E_a / m_{P'})^{1/2} \cos\theta)^2} \quad (8)$$

where it is the fragment  $a$  which flies away and the fragment  $b$  which fuses with the other nucleus,  $E_a$  and  $E_b$  are their kinetic energies,  $B_{P'}$  is the binding energy of  $a$  and  $b$  in  $P$ ,  $\mu$  is the reduced mass of the system  $a+b$ ,  $m_{P'}$ ,  $m_a$ ,  $m_b$  are the masses of  $P'$ ,  $a$ ,  $b$  and  $\theta$  is the emission angle of  $a$  with respect to the direction of  $P'$ . The kinetic energy and angle of a hot fragment are determined using energy and momentum conservation laws. An intrinsic angular momentum is calculated using a mean radial distance and momentum of the participant zone relative to the capturing spectator in the configuration of minimum distance between the projectile and target.

In order to describe also the inverse kinematics, namely when the projectile is heavier than the target, the system is transformed into the inverse frame where the projectile becomes a target and

vice versa. Then the calculation proceeds as described above and the final kinematic properties of the reaction products are obtained after a re-transformation into the lab frame.

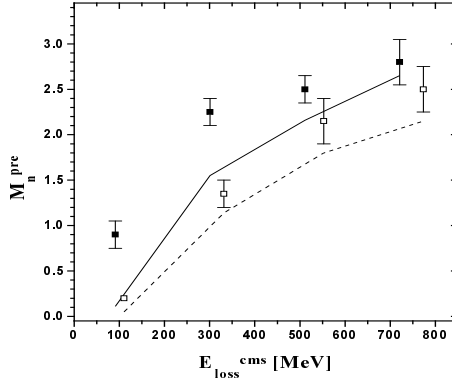


Figure 1: Experimental [21] ( symbols ) and calculated ( lines ) mean multiplicities of pre-equilibrium neutrons as a function of kinetic energy loss of the projectile-like fragment. Solid squares - experimental multiplicities measured in reaction of 35 MeV/nucleon  $^{48}\text{Ca}$  beam with  $^{112}\text{Sn}$  target, open squares - ditto for 35 MeV/nucleon  $^{40}\text{Ca}$  beam, solid line - calculated multiplicities in reaction of 35 MeV/nucleon  $^{48}\text{Ca}$  beam with  $^{112}\text{Sn}$  target, dashed line - ditto for 35 MeV/nucleon  $^{40}\text{Ca}$  beam.

The model of pre-equilibrium emission was compared to available experimental data. The multiplicities of the pre-equilibrium emission were compared to the results of work [21] where a multiplicity of the pre-equilibrium particles was determined in coincidence with projectile-like fragments ( PLFs ) in the reactions of Ca beams with  $^{112}\text{Sn}$  target at 35 MeV/nucleon. In Fig. 1 are given the values of pre-equilibrium neutron multiplicity in reaction  $^{40,48}\text{Ca} + ^{112}\text{Sn}$  for several bins of kinetic energy loss of the projectile-like fragment. The solid ( open ) squares represent the results of work [21] and the lines represent the results of the calculation. The agreement is quite good. The parameters  $\sigma=0.25$  and  $\kappa=0.3$  were used in the calculation. The same values of  $\sigma$  and  $\kappa$  were tested in other reactions and lead to results which track well with the results of experimental works where multiplicities of pre-equilibrium particles were determined in coincidence with heavy residues or fission fragments [22, 7] or in coincidence with the quasi-projectile [12].

In the recent experimental work [23] a linear correlation between the primary mass of the projectile-like fragment and the net mass loss due to the de-excitation was reported in the nearly symmetric reactions of  $^{93}\text{Nb}$  with  $^{116}\text{Sn}$  at 25 MeV/nucleon in both normal and inverse kinematics for different dissipation bins. The net mass loss increases with the primary mass of the projectile-like fragment. With increasing dissipation this trend occurs in the still broader range of primary masses. Since the net mass loss is possibly correlated to the excitation energy of the hot primary projectile-like nucleus, one may expect similar trend also for excitation energy. Such a trend is a possible signal of the breakdown of the concept of deep inelastic transfer. In Fig. 2 is given a calculated correlation between the excitation energy and the mass of the hot projectile-like nucleus for different bins of kinetic energy. One can see that the calculation follows the experimental trend. At masses close to the beam the deep inelastic transfer takes place but the range of primary masses is quite narrow. To achieve larger mass change a more violent collision should occur. When the target strips a part of the projectile, the projectile-like fragment remains relatively cold. Hot projectile-like fragments are produced if a part of the target is picked-up by the projectile.

The production of heavy residues was studied recently by Skulski et al. [24] in the reaction  $^{86}\text{Kr} + ^{197}\text{Au}$  at projectile energy 35 MeV/nucleon. A spectrum of kinetic energies of the target-like

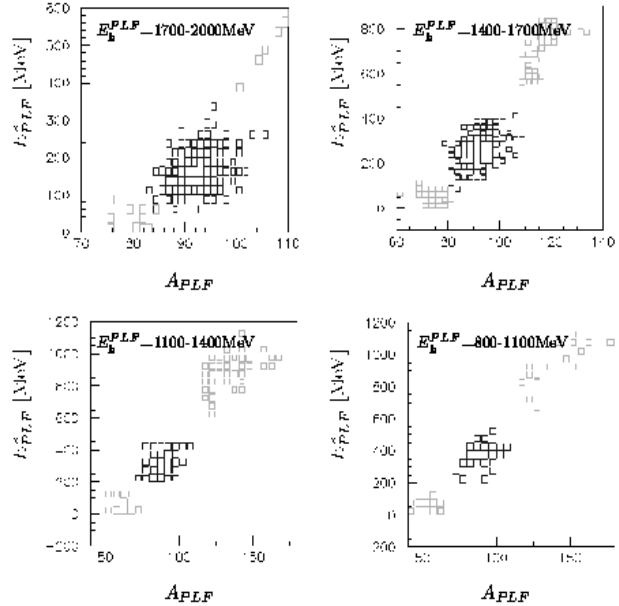


Figure 2: Calculated correlation between the primary mass and the excitation energy of a projectile-like fragment in the reaction  $^{93}\text{Nb}$  with  $^{116}\text{Sn}$  at 25 MeV/nucleon. Four different bins of  $E_k^{\text{PLF}}$  are defined. Black squares - PE+DIT events, grey squares - PE+RGF events.

fragments ( TLFs ) was measured at angles  $9^\circ - 46^\circ$  in coincidence with projectile-like fragments with  $Z \geq 25$  at angles  $2^\circ - 8^\circ$ . The spectrum exhibits two humps, one of them is the low energy component at energies below 40 MeV and the second one is located between 50 and 100 MeV. Fig. 3a shows the calculated spectrum of kinetic energies for the same reaction using identical angle cuts and charge threshold. One can see that similar range of the kinetic energies is covered. The double-humped structure is not as clearly pronounced as in the experiment. As may be seen in Fig. 3b, the double-humped shape can be explained by a correlation between the kinetic energy and the angle. The low energy particles are emitted at large angles and an additional energy losses or rescattering can be caused by interaction with the target. The high energy part is possibly influenced by decreasing mass and charge and increasing excitation energy of the coincident projectile-like fragment what leads to the decrease of detection probability because of the charge threshold.

The production of heavy residues in inverse kinematics was measured recently by Souliotis et al. [25] in the reaction  $^{197}\text{Au} + ^{nat}\text{Ti}$  at projectile energy 20 MeV/nucleon. Fig. 4 shows the measured yields of heavy residues at the forward angles as a function of  $A$  and  $Z$ . The solid line represents the calculated centroids of  $Z$  for a given residue mass. The code GEMINI [26] was used for the de-excitation stage. One can see that the calculation follows the experimental trend quite well. In this case the participant zone sticks almost exclusively to the heavy projectile. An introduction of the incomplete fusion leads to the production of neutron-deficient residues with masses close to the beam. Such behavior can not be explained by deep inelastic transfer only.

The measurement of the production of intermediate mass fragments ( IMFs ) in symmetric collisions  $^{58}\text{Fe}, ^{58}\text{Ni} + ^{58}\text{Fe}, ^{58}\text{Ni}$  at 30 MeV/u [27] determined three different sources of IMFs, the moderately excited projectile(target)-like source at velocities near the projectile (target) and the highly excited source at velocities near the center of mass velocity. Fig. 5 shows a correlation between the excitation energy and the velocity of reaction products in the lab frame. Both projectile-like and target-like nuclei are included in the plot. One can identify three sources analogous to the ones seen

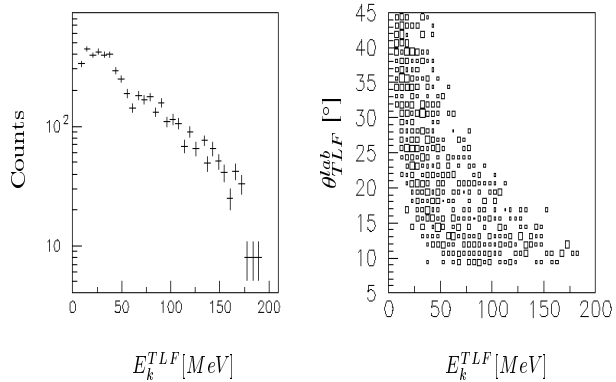


Figure 3: Calculated kinetic energy spectrum of target-like fragments in reaction  $^{86}\text{Kr} + ^{197}\text{Au}$  at projectile energy 35 MeV/nucleon and the correlation of  $\theta_{TLF}$  and  $E_k^{TLF}$  for the same reaction. For details see text.

in experiment. The projectile- and target-like sources are moderately excited. The third source with the average velocity close to the mid-velocity is highly excited. Both the PLFs and TLFs are included in this source. The difference of the average isospin of IMFs from different sources which was experimentally observed may possibly be explained by the difference in the excitation energy of the sources, since the isospin dependences of isotopic ratios become flatter at high excitations, as follows from refs. [28, 29].

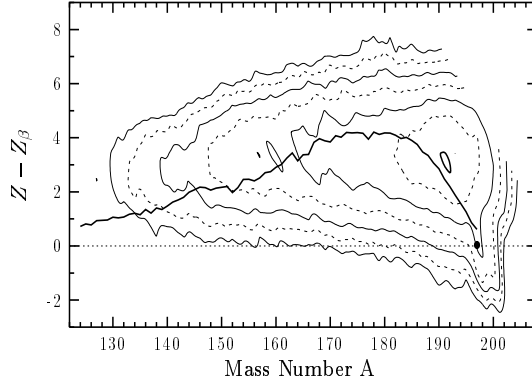


Figure 4: Measured yields [25] of heavy residues at the forward angles in the reaction  $^{197}\text{Au}(20 \text{ MeV/nucleon}) + ^{nat}\text{Ti}$  as a function of A and Z. Z is expressed relative to the line of  $\beta$ -stability. Solid line - calculated centroids of the fragment charge for given residue mass (the code GEMINI [26] was used for de-excitation ).

The comparison to the broad range of experimental observables measured in various reactions in the Fermi energy domain appears to imply that the present approach describes correctly the processes leading to the production of excited projectile-like and target-like nuclei in the range between 20 and 50 MeV/nucleon. With increasing projectile energy, the production of three-body events and the compression phenomena start to play an important role. As a primary candidates for three-body events can be considered hot fragments where the relative motion of the participant zone leads to values of intrinsic angular momenta above the critical angular momentum for fusion. The compression phenomena can primarily take place in the events where the fragment with the mass close to the compound nucleus is produced with low intrinsic angular momentum.

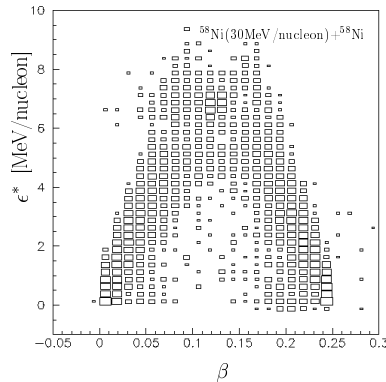


Figure 5: Calculated correlation of the excitation energy and velocity of the hot nuclei produced in the reaction  $^{58}\text{Ni} + ^{58}\text{Ni}$  at 30 MeV/nucleon.

In conclusion, the approach presented in the present work appears to be a suitable tool to describe the production of hot nuclei which later undergo multifragmentation. Furthermore, production of rare beams in the Fermi energy domain can be addressed using this approach ( for instance, experimental studies are underway at the Cyclotron Institute of Texas A&M University [30] ).

The author would like to thank to G.A. Souliotis and S.J. Yennello for support and fruitful and stimulating discussions. This work was supported in part by the NSF through grant No. PHY-9457376, the Robert A. Welch Foundation through grant No. A-1266, and the Department of Energy through grant No. DE-FG03-93ER40773. M. V. was also supported through grant VEGA-2/5121/98.

## References

- [1] C. Gregoire and B. Tamain: Ann. Phys. Fr. **11**, 323 (1986).
- [2] J. Pochodzalla: Prog. Part. Nucl. Phys. **39**, 443 (1997).
- [3] H. Feldmeier and J. Schnack: Rev. Mod. Phys. **72**, 655 (2000).
- [4] J.J. Griffin: Phys. Rev. Lett. **17**, 478 (1966).
- [5] G. Harp, J. Miller, and B.J. Berne: Phys. Rev. **165**, 1166 (1968).
- [6] J. Randrup and R. Vandenbosch: Nucl. Phys. A **474**, 219 (1987).
- [7] M. Veselsky *et al.*: Z. Phys. A **356**, 403 (1997).
- [8] M. Böhning: Nucl. Phys. A **152**, 529 (1970).
- [9] H. Fuchs and K. Möhring: Rep. Prog. Phys. **57**, 231 (1994).
- [10] D.J. Parker *et al.*: Phys. Rev. C **44**, 1528 (1991).
- [11] L. Tassan-Got and C. Stéfan, Nucl. Phys A **524**, 121 (1991).
- [12] M. Veselsky *et al.*: accepted to Phys. Rev. C, [nucl-ex/0002007](https://arxiv.org/abs/nucl-ex/0002007).

- [13] F.P. Heßberger *et al.*: Z. Phys. A **348**, 301 (1994).
- [14] J. Wilczynski *et al.*: Nucl. Phys. A **373**, 109 (1982).
- [15] L.E. Tubbs *et al.*: Phys. Rev. C **32**, 214 (1985).
- [16] J. Wilczynski: Nucl.Phys. A **216**, 386 (1973).
- [17] J. Gosset *et al.*: Phys.Rev. C **16**, 629 (1977).
- [18] W.A. Friedman: Phys. Rev. C **27**, 569 (1983).
- [19] J.-J. Gaimard and K.-H. Schmidt: Nucl. Phys. A **531**, 709 (1991).
- [20] N. Matsuoka *et al.*: Nucl. Phys. A **311**, 173 (1978).
- [21] D.K. Agnihotri *et al.*: Adv. Nucl. Dyn. 1997, 3, 67.
- [22] E. Holub *et al.*: Phys. Rev. C **28**, 252 (1983).
- [23] G. Casini *et al.*: **nucl-ex/0010001**.
- [24] W. Skulski *et al.*: Phys. Rev. C **53**, R2594 (1996).
- [25] G.A. Souliotis *et al.*: in preparation, see also G.A. Souliotis *et al.*: Phys. Rev. C **57**, 3129 (1998).
- [26] R. J. Charity *et al.*: Nucl. Phys. A **483**, 371 (1988).
- [27] E. Ramakrishnan *et al.*: Phys. Rev. C **57**, 1803 (1998).
- [28] M. Veselsky *et al.*: Phys. Rev. C **62**, 41605 (2000).
- [29] M. Veselsky *et al.*: submitted to Phys. Lett. B, **nucl-ex/0003004**.
- [30] G.A. Souliotis *et al.*: internal communication of the Cyclotron Institute.